Supporting Information

Staquicini et al. 10.1073/pnas.1114503108

SI Materials and Methods

Reagents. The following reagents were used: mouse monoclonal anti-PR-3 antibody (Lab Vision and Accurate Chemicals); goat anti-RAGE IgG (R&D Systems), goat anti-ANXA2 IgG (Santa Cruz Biotechnology), and goat anti-GST IgG (Amersham Biosciences); rabbit antiprohibitin IgG (Research Diagnostics), rabbit anticaveolin-1 IgG (Santa Cruz Biotechnology), rabbit anti-ANXA4 IgG (Abcam), rabbit anti-ApoE3 IgG (Abcam) and rabbit antiintegrin α4 subunit IgG (Novus Biologicals). Secondary antibodies used were as follows: rat and goat antirabbit (BioRad) or rat antigoat (Promega) alkaline phosphatase-conjugated IgG; goat antirabbit horseradish peroxidase (HRP)-conjugated IgG (Sigma), and rabbit antihuman HRP-conjugated IgG (Sigma). The following recombinant proteins were used: His_6-ANXA2 and A5 (AmProx), stem cell growth factor alpha (SCGF-alpha) (Cell Sciences), ANXA4, ANXA1, and ANXA5 (Novus Biologicals), PR-3 (Sigma), and RAGE-Fc and BMPRIA-Fc (R&D Systems), ApoE3, ApoE4, ApoC, and cathepsin B (Sigma), VEGFR (R&D Systems), integrin α4 subunit (Novus Biologicals), and human integrin αvβ5, α5β1 and αvβ3 (Millipore). GST-prohibitin was a gift from Dr. Srikumar Chellappan (H. Lee Moffitt Cancer Center & Research Institute). Human placentas were purchased from ILSbio. Human paraffin-embedded tissue samples (prostate, brain, fat, skin, and muscle) were obtained either from ILSbio or from an institution-banked panel of formalin-fixed samples (David H. Koch Center, University of Texas M. D. Anderson Cancer Center).

Patient Selection and Clinical Course. This study adheres strictly to current medical ethics recommendations and guidelines regarding human research, and it has been reviewed and approved by the Clinical Ethics Service, the Institutional Biohazard Committee, Clinical Research Committee, and the Institutional Review Board of the University of Texas M. D. Anderson Cancer Center.

Patient #1 entered in the study was a 48-year-old caucasian man with Waldenström macroglobulinemia who met the formal criteria for brain-based determination of death (1, 2). Clinical attributes and detailed course of this human subject were reported elsewhere (3).

Patient #2 was a 66-year-old caucasian man that presented with castration-resistant prostate cancer and predominant bone metastases. The primary tumor was diagnosed as a Gleason Score $10(5+5)$ prostate cancer, six years prior to study entry. Over his clinical course, the patient was treated with combined androgen ablation with the luteinizing hormone-releasing hormone (LHRH) antagonist leuprolide plus the antiandrogen bicalutamide. Several regimens of systemic chemo-hormonal therapy (ketoconazole plus doxorubicin alternating with viblastine plus estramustine; cyclophosphamide, vincristine, plus dexamethasone; docetaxel plus carboplatinum; and paclitaxel plus diethylstilbestrol or thalidomide; vinorelbine; mitoxantrone; PC-SPES), radiopharmaceutical therapy (Strontium-89), and targeted therapy with a proteasome inhibitor (bortezomib) were given sequentially over time. Patient #2 also underwent courses of external beam radiation therapy for bone pain palliation in the neck (3,000 cGray, C1-T2) and pelvic (3,000 cGray, L2-S1) metastatic sites. Ultimately, Patient#2 presented to the emergency room with respiratory and cardiovascular failure secondary to worsening pleural effusion and hemothorax. Despite thoracocentesis, endotracheal intubation, mechanical ventilation, and full medical support in an intensive care unit setting, he evolved into multiple organ failure. Based on his irreversible clinical condition, a terminal wean from life-support systems was planned in accordance to previously stated patient wishes. After discussion with the family and a surrogate informed written consent was obtained from legal next-of-kin, the patient was enrolled in the study.

Patient #3 was a 73-year-old caucasian man that presented with locally advanced prostate cancer. At two years prior to study entry, he was diagnosed with Gleason Score $9(4+5)$ prostate cancer and treated with integrated external bean radiation therapy plus brachytherapy implants and long-term androgen ablation with the LHRH antagonist leuprolide. He subsequently developed castration-resistant prostate cancer with predominant bone metastases. He was treated with systemic chemotherapy (docetaxel plus prednisone) and a course of external beam radiation therapy for palliation of bone metastasis pain in the lumbar spine (3,000 cGray, L1-L5). Previously to the diagnosis of prostate cancer, the patient had been successfully treated for a non-Hodgkin lymphoma (diffuse large cell type involving head and neck) with systemic chemoimmunotherapy (cyclophosphamide, doxorubicin, vincristine, prednisone, and rituximab) plus mantle radiation therapy. After nine years, at the time of study entry, he had no clinical or laboratory evidence of lymphoma and was presumably cured from that tumor. Patient #3 had multiple comorbidities including arterial hypertension, coronary artery disease (status post several coronary artery bypass graft surgeries and vascular stent insertion procedures), plus radiation-induced lung fibrosis. During an inpatient admission for worsening chest and abdominal pain, he developed severe acute respiratory distress syndrome and was transferred to the intensive care unit but became critically ill and unresponsive under prolonged endotracheal intubation and mechanical ventilation. Based on this clinically irreversible condition, a terminal wean from life-support systems was requested. Thus, after informed written consent was obtained from the patient and the legal next-of-kin, the patient was enrolled in the study.

Administration of Phage Display Library and Sample Collection. Endotoxin levels of administered random peptide libraries were assessed with Endosafe (Charles River). Short-term intravenous infusion of phage display sublibrary recovered from the first, second, and third rounds of selection (3) [2×10^{12} transducing units (TU) from each organ; total 10^{13} TU pooled] were followed by multiple representative tissue biopsies. Prostate, liver, and metastatic tumor samples were obtained by needle biopsy under ultrasonographic guidance; skin, adipose tissue, and skeletal muscle samples were obtained surgically. Bone marrow needle aspirates and core biopsy samples were also obtained. After systemic delivery of a naïve phage-displayed random peptide library to the first human subject (3), ligand phage populations were recovered, pooled, and serially screened in the two subsequent patients.

Postbiopsy Processing of Human Tissue Samples. Universal precautions were used by the laboratory personnel handling human samples. The amount of phage present in each tissue was determined by either TU-counting (3, 4) and/or quantitative real-time PCR (5). The PCR reaction admixture consisted of 60 ng of total DNA, Power SYBR Green PCR Master Mix (Applied Biosystems), and 3.75 picomoles of oligonucleotide primers directed to the amplification of a fragment of the fUSE5 *pIII* gene. For each experiment, standard curves were generated with serial dilutions of phage plasmid, from 2.4×10^2 to 2.4×10^6 copies. Each point on the curve, as well as each tissue sample of DNA, was determined in triplicates. A standard calibration curve was calculated

by the Applied Biosystems 7500 Fast System SDS software (version 1.3.1.21, Applied Biosystems) through regression of the crossing points of the PCR curves from plasmid dilutions. The number of viral particles in each DNA sample was determined by comparison of the amplification threshold for each sample to the standard curve. The amplification efficiency (AE) of each PCR cycle was calculated from the slope (s) of the standard curve through the equation $AE = 10^{1/(-s)}$. All amplifications and calculations were performed with an ABI7500 Fast system (Applied Biosystems). For large-scale sequencing, total DNA was extracted and used for PCR amplification of phage inserts. The amplicons produced from tissues and the CX_7C library were subsequently purified and sequenced with a pyrosequencing approach (FLX platform, Roche/454).

Statistical Analysis. One-sided Fisher's exact test was used to identify tripeptide motifs significantly enriched after three rounds of selection, for each targeted tissue, and for comparison to the parental unselected random peptide library. A Monte Carlo algorithm (6) was applied to minimize the number of assumptions, and to account for the large number of comparisons made for each round. Simulations were generated and a "computational staining plot" was produced for each targeted tissue at each round of selection, after comparison to the random peptide library and to unrelated tissues. Analysis of peptide sequences was executed with a character pattern recognition program based on SAS (version 8.1.2; SAS Institute) and Perl (version 5.8.1). To identify peptide similarities to human proteins, we codified Peptide Match software in Perl 5.8.1 based on RELIC (3). Peptide-protein similarity scores for each residue were calculated based on a modified BLOSUM62 substitution matrix.

Peptide Synthesis and Antibody Production. The peptides CWELGGGPC, CPGGGLVHC, CKGGRAKDC, CMRGFRAAC, CMGGHGWGC, and a negative control peptide (sequence CARAC, unless otherwise specified) were chemically synthesized, cyclized, tagged on the N terminus with biotin or KLH, and purified by high-performance liquid chromatography (HPLC) by commercial vendors (AnaSpec, Genemed Synthesis, PolyPeptide Laboratories, or Sigma). Antisera against cyclized KLH-conjugated peptides were produced in rabbits.

Protein Extraction and Peptide Affinity Chromatography. Human tissue samples were homogenized in ice-cold tris-buffered saline (TBS) supplemented with 100 mM phenylmethylsulfonyl fluoride (PMSF). Following extensive washes, tissue pellets were resuspended in extraction buffer (TBS containing 100 mM octylglucoside, 100 mM PMSF, 10 mM $CaCl_2$, and 10 mM $MgCl_2$), and protein extraction was carried out overnight (ON) at 4 °C. Membrane proteins of human white mononuclear bone marrow cells were purified on a Ficoll gradient. Isolation of membrane proteins from white adipose tissue (WAT) and their separation into caveolar and noncaveolar lipid raft fractions were based on established protocols (7). Extracted proteins were chromatographed on affinity columns (Pierce) previously conjugated with each synthetic peptide of interest. Columns were washed extensively and were eluted with a solution of the corresponding peptide followed by a low pH buffer (extraction buffer supplemented with 0.1 M glycine and 0.1 M NaCl, pH 2.5). Fractions of 0.5 mL were collected, and those containing protein (O.D. 280 nm) were used for further studies.

Mass Spectrometry. Protein identification was carried out through a Nano LC-MS/MS peptide sequencing technology (ProtTech). In brief, each protein gel band was destained, cleaned, and digested in-gel with sequencing grade modified trypsin. The resulted peptide mixture was analyzed by a LC-MS/MS system, in which a HPLC with a 75 μm inner diameter reverse-phase C18 column was on-line coupled to an ion-trap mass spectrometer. The mass spectrometric data acquired were used to search a nonredundant protein database. The output from the database search was manually validated before reporting. The following peptides were identified: ANXA4, GLGTDEDAIISVLAYRN and GLGTDDNTLIRV; ApoE3, SELEEQLTPVAEETRA and AATVGSLAGQPLQER; PR-3, LFPDFFTRVAYVDWIR, LVNVVLGAHNVRTQEPTQQHFSVAQVFLNNYDAENK, and IVGGHEAQPHSRPYMASLQMR.

Protein Microarray Screening. High-density arrays of the protein expression set of the hEx1 library were commercially obtained (imaGenes). For rabbit antipeptide serum profiling, the filters were blocked in 2% (wt/vol) nonfat, dry milk powder in TBST [TBS containing 0.1% (vol/vol) Tween-20] for 2 h, washed twice in TBST, and subsequently incubated with antipeptide serum diluted 1:1,000 for 16 h. Following three 30 min TBST washes and subsequent incubation with the secondary antibody (anti-rabbit-IgG-alkaline phosphatase, Sigma) at 1:5,000 dilution in 2% (wt/vol) milk/TBST, the filters were washed three times in TBST-T for 20 min each, followed by a 10 min wash in TBS and a further wash for 10 min in alkaline phosphatase buffer (1 mM $MgCl_2$, 0.1 M Tris pH 9.5), and subsequent incubation in 25 mM Attophos (Roche) in alkaline phosphatase buffer for 5 min. The filters were illuminated with long-wave ultraviolet light, and the images were taken with a high-resolution CCD detection system (Fuji). Image analysis was performed with VisualGrid (GPC Biotech). Positive clone cDNA inserts were amplified and sequenced for identity confirmation of expressed proteins.

Phage Binding Assays. Binding of targeted phage to immobilized candidate receptors was evaluated as described (8). Micro-wells of 96-well plates were blocked with phosphate-buffered saline (PBS) containing 3% BSA, washed, and incubated with 10^9 TU of targeted phage. Inhibition of phage binding was performed in the presence of increasing concentrations of synthetic peptides, as indicated. For phage display screening on immobilized prohibitin, 10^9 TU of phage clones recovered from the second round of in vivo selection were incubated ON with 1 μg of immobilized recombinant GST-prohibitin. Bound phage were recovered by infection of host bacteria (*Escherichia coli* K91 Kan).

Protein Binding Assays. Titration of antipeptide antibodies was performed on Maxisorb Immunoplates (Nunc) coated with 1 μg/mL of peptides or proteins. Incubation with primary antibodies was followed by signal detection with goat anti-rabbit HRP-conjugated IgG (Sigma) and 3, 3′, 5, 5′-tetramethylbenzidine (TMB) (Calbiochem). To evaluate protein-protein interactions, we performed ELISA on 96-well plates coated with 1 μg/mL of recombinant candidate receptors, as indicated. Blocking of exposed nonspecific binding sites was performed with PBS containing either 2% gelatin or 1% BSA, as indicated. Ligand candidates were added to the wells at different concentrations, as indicated. Specific binding was detected by incubation with appropriate primary and secondary antibodies. For capture experiments, immobilized His_6-ANXA2 and ANXA5 were incubated with recombinant GST-prohibitin. Protein interaction, assessed by immunoblotting with anti-GST antibody, was detected with anti-rabbit or antigoat secondary alkaline phosphatase-conjugated polyclonal antibodies.

Immunostaining. Immunohistochemical staining of normal human TMAs (CelleStan) was performed as follows. After complete removal of paraffin and antigen retrieval in high pH, slides were incubated with primary antibodies followed by appropriate HRP-conjugated secondary antibodies (EnVision DakoCytomation or Vector). High-resolution pictures were obtained with ImageScope (Aperio). Immunohistochemical staining of bone marrow

and prostate cancer specimens was performed on 4 μm sections and carried out either in an Autostainer or manually. When required, antigen retrieval was performed with target retrieval solution (Dako). Tissue sections were incubated with primary antibody for 1 h, and the reactions were developed with either the labeled streptavidin-biotin (LSAB) system or the EnVision kit (Dako). Sections were counterstained with hematoxylin (Biocare Medical).

1. Pentz RD, Flamm AL, Pasqualini R, Logothetis CJ, Arap W (2003) Revisiting technical guidelines for research with terminal wean and brain-dead patients. *Hastings Cent Rep* 33:20–26.
2. Pentz RD, et al. (2005) Ethics guidelines for research with the recently dead. *Nat Med* 11:1145–1149.
3. Arap W, et al. (2002) Steps toward mapping the human vasculature by phage display. *Nat Med* 8:121–127.
4. Pasqualini R, Ruoslahti E (1996) Organ targeting in vivo using phage display peptide libraries. *Nature* 380:364–366.
5. Kolonin MG, et al. (2006) Ligand-directed surface profiling of human cancer cells with combinatorial peptide libraries *Cancer Res* 66:34–40.
6. Kolonin MG, et al. (2006) Synchronous selection of homing peptides for multiple tissues by in vivo phage display. *FASEB J* 20:979–981.
7. Smart EJ, Ying YS, Mineo C, Anderson RG (1995) A detergent-free method for purifying caveolae membrane from tissue culture cells. *Proc Natl Acad Sci USA* 92:10104–10108.
8. Dias-Neto E, et al. (2009) Next-generation phage display: integrating and comparing available molecular tools to enable cost-effective high-throughput analysis. *PLoS One* 4:1–11.

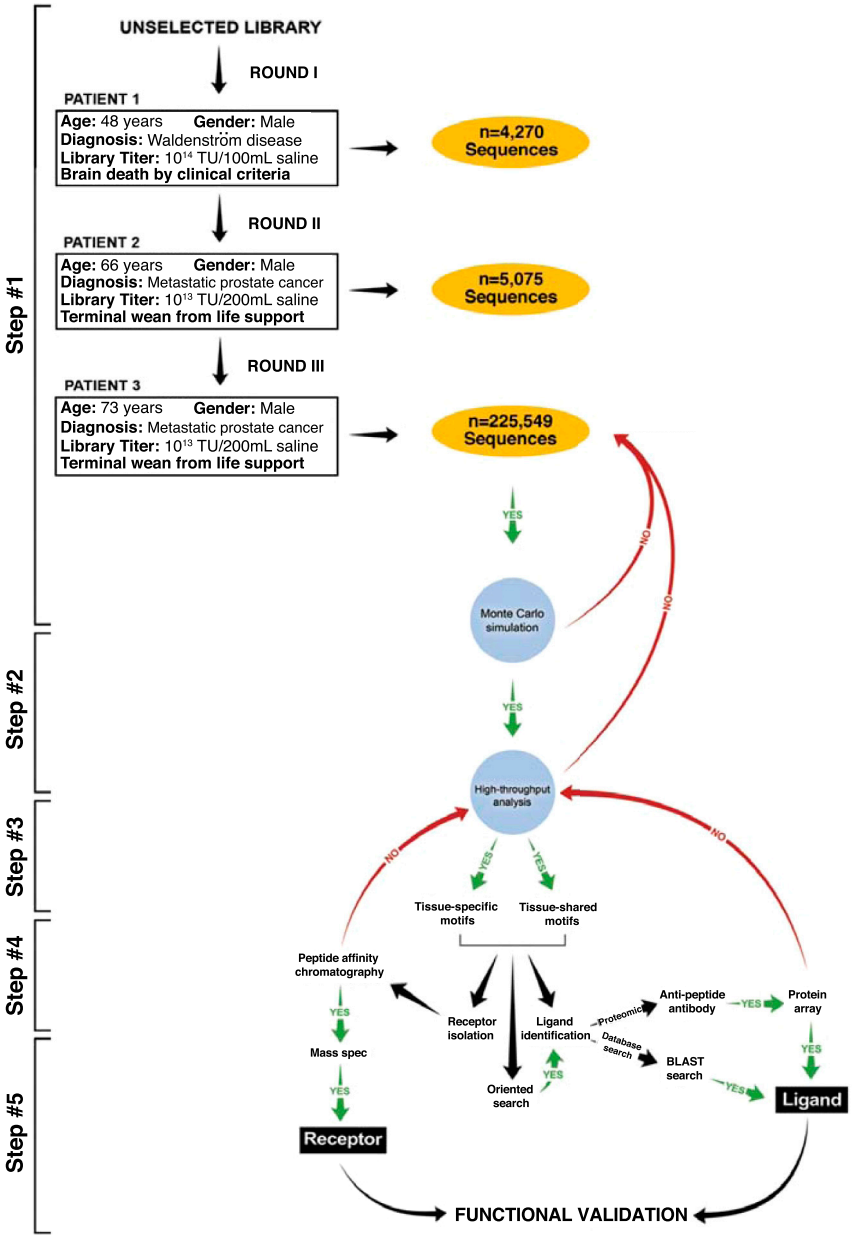

Fig. S1. The schema represents the approach used for the isolation of shared and tissue-specific ligand peptides in cancer patients. Step #1: three serial rounds of combinatorial selection were performed as indicated. Sequencing of DNA inserts encoding the displayed peptides provided the total number of peptides recovered in each round. Step #2: Monte Carlo simulations and high-throughput tripeptide motif analyses were used to evaluate positive selection of peptides compared to the random peptide library. Step #3: shared and tissue-specific ligand peptide candidates were selected based on the analyses performed in Step #2. Step #4: biostatistical analysis is followed by ligand identification and receptor isolation. Steps #5: functional validation of the candidate ligand-receptor systems is performed at the protein, cell, and tissue levels.

A

Annexin A4

MAMATKGGTVKAASGFNAMEDAQTLRKAMKGLGTDEDA
IISVLAYRNTAQRQEIRTAYKSTIGRDLIDDLKSELSG
NFEQVIVGMMTPTVLYDVQELRRAMKGAGTDEGCLIEI
LASRTPEEIRRISQTYQQQYGRSLEDDIRSDTSFMFQR
VLVSLSAGGRDEGNYLDDALVRQDAQDLYEAGEKKWGT
DEVKFLTVLCSRNRNHLLHVFDEYKRISQKDIEQSIKS
ETSGSFEDALLAIVKCMRNKSAYFAEKLYKSMKGLGTD
DNTLIRVMVSRAEIDMLDIRAHFKRLYGKSLYSFIKGD
TSGDYRKVLLVLCGGDD

C

Apolipoprotein E3

MKVLWAALLVTFLAGCQAKVEQAVETEPEPELRQQTEW
QSGQRWELALGRFWDYLRWVQTLSEQVQEELLSSQVTQ
ELRALMDETMKELKAYKSELEEQLTPVAEETRARLSKE
LQAAQARLGADMEDVRGRLVQYRGEVQAMLGQSTEELR
VRLASHLRKLRKRLLRDADDLQKRLAVYQAGAREGAER
GLSAIRERLGPLVEQGRVRAATVGSLAGQPLQERAQAW
GERLRARMEEMGSRTRDRLDEVKEQVAEVRAKLEEQAQ
QIRLQAEAFQARLKSWFEPLVEDMQRQWAGLVEKVQAA
VGTSAAPVPSDNH

B

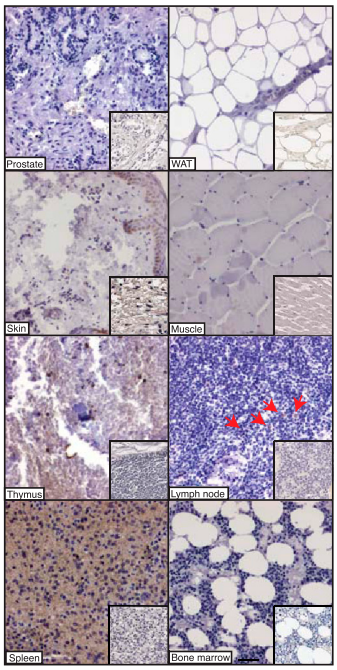

Fig. S2. (*A*) LC-MS/MS of peptides matching the candidate receptor ANXA4. Peptides identified are highlighted in yellow. (*B*) Immunostaining of sections of normal human tissue with an anti-α4 integrin subunit antibody. Arrows point to α4-subunit positive lymphocytes. (Scale bar, 100 μm.) (*C*) LC-MS/MS of peptides matching the candidate receptor ApoE3. Peptides identified are highlighted in yellow.

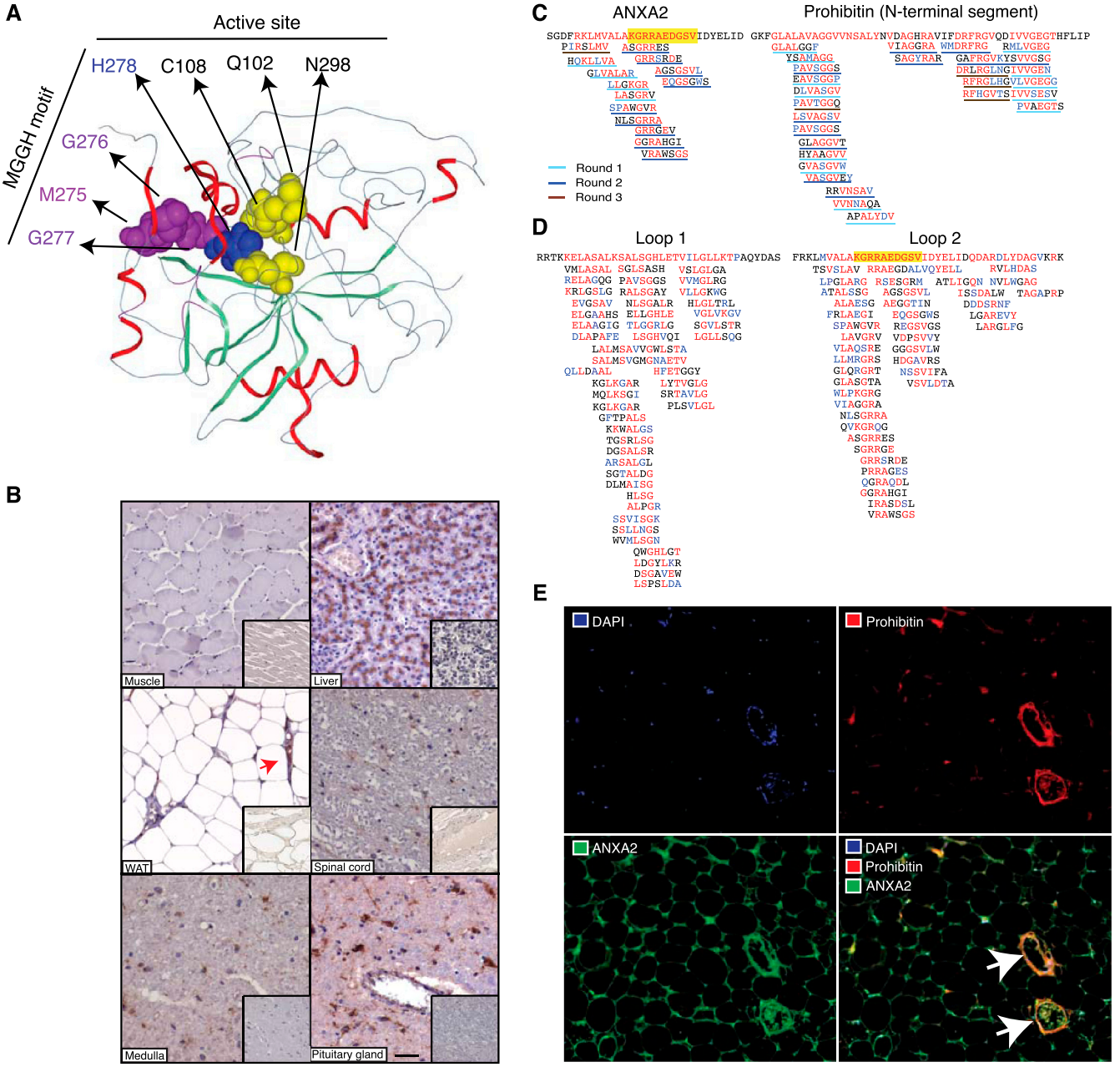

Fig. S3. (*A*) Molecular Modeling of Cathepsin B. The surface-exposed MGGH motif and the amino acid residues composing the active site of cathepsin B are indicated. (*B*) Immunostaining of sections of normal human tissue with an anticathepsin B antibody. Arrows point to a cathepsin B positive blood vessel. (Scale bar, 100 μm.) (*C*) Left box: peptides enriched in three rounds of selection in human WAT matched to the ANXA2 amino acid sequence. Underlining colors indicate the original round of selection. The CKGGRAKDC similarity sequence is highlighted in yellow. Right box: peptides enriched in WAT matched to prohibitin. Similarity criteria: four or more amino acids identical (red) or conserved (blue) to the correspondingly positioned protein residues. (*D*) ANXA2 surface-exposed connector loops. Peptides enriched in WAT are shown. (*E*) Colocalization of ANXA2 and prohibitin in the vasculature of WAT. Arrows point to blood vessels positively stained for ANXA2 (green) and prohibitin (red). DAPI (blue) indicates nuclear staining.

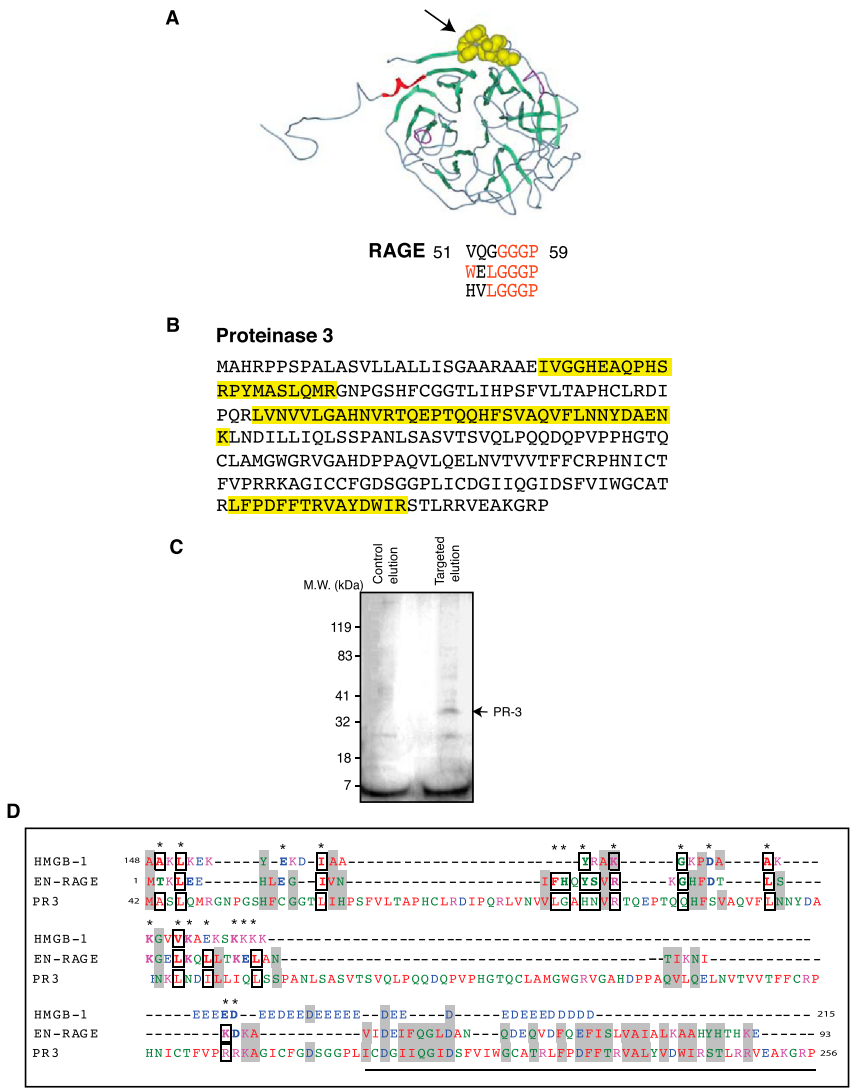

Fig. S4. Identification of the protein complex RAGE/leukocyte proteinase-3 as a molecular target of bone metastases. (*A*) Molecular modeling of the RAGE extracellular domain. Shown is the ribbon secondary structure conformation of RAGE. The surface-exposed WKLGGGP sequence is indicated (arrow). Similarity of bone marrow-homing peptide to the human receptor is shown. (*B*) LC-MS/MS of peptides matching the candidate receptor PR-3. Peptides identified are highlighted in yellow. (*C*) Isolation of PR-3 as a bone marrow target for the RAGE-like motif. Monoavidin beads loaded with biotinylated synthetic peptides: a negative control peptide (sequence CARAC; indicated as control elution) or an equimolar admixture of CWELGGGPC plus CPGGGLVHC (indicated as targeted elution), were incubated sequentially with a membrane protein extract from human white mononuclear bone marrow cells, washed, eluted by low pH, resolved by SDS-PAGE, and stained with Coomassie blue. Arrow: ~35 kDa band specific to the RAGE-like peptides. (*D*) Similarity of human PR-3 to human EN-RAGE and human HMGB1. Asterisks mark residues critical for RAGE binding to either HMGB1 or EN-RAGE. Residues conserved between PR-3 and either HMGB1 or EN-RAGE are highlighted. Residues that are both critical for RAGE binding to HMGB1 or EN-RAGE and conserved between PR-3 and either HMGB1 or EN-RAGE are boxed. Amino acid residue color-coding: red, hydrophobic; green, neutral and polar; purple, basic; blue, acidic. The α-helix within the PR-3 C-terminus is underlined.

Table S1. Homing of peptide motifs to human tissues

Target organ/ motif	Round 3		Round 2		Round 1			Round 3 (pyrosequencing)		
	P-value (vs. library)	*P*-value (vs. other tissues)	*P*-value (vs. library)	*P*-value (vs. other tissues)	*P*-value (vs. library)	*P* -value (vs. other tissues)	Motif frequency (%) Round 3	*P*-value (vs. library)	*P*-value (vs. other tissues)	Motif frequency (%) Round 3
Bone marrow										
OGW*	0.0076	0.0264	0.4409	0.6871	1.0000	1.0000	1.3	6.84E−06	0.98	0.11
GIL*	0.0076	0.0194	0.2927	0.9995	0.5387	0.8153	1.3	0	0	0.99
GEM*	0.0111	0.0132	0.1290	0.1031	0.1563	0.2047	1.2	4.2736E−58	6.06954E−09	0.11
ILL*	0.0111	0.0058	0.4409	0.9992	0.5387	0.4052	1.2	0	0	0.97
ATG*	0.0205	0.0023	0.1008	0.3513	0.3726	0.7034	1.5	1.594E−62	2.66701E−40	0.27
QGS*	0.0205	0.0009	0.5879	0.5865	1.0000	1.0000	1.5	2.4759E−30	3.19911E−10	0.15
EGS*	0.0282	0.0144	0.2584	0.4893	0.7873	0.8902	1.4	1.2602E−27	8.29897E−30	0.18
HVS*	0.0342	0.0335	0.4409	0.6871	0.2902	0.3015	0.9	9.1586E−60	5.622E−18	0.21
HAR*	0.0342	0.0089	0.2927	0.5429	1.0000	1.0000	0.9	1	1	0.09
RWS*	0.0478	0.0148	0.9621	0.9677	0.0874	0.0158	1.6	8.0902E−58	3.295E−66	0.34
GPM*	0.0498	0.0201	0.0856	0.1973	1.0000	1.0000	0.8	4.2019E−23	3.25583E−07	0.09
GGG*	0.0413	0.0982	0.0750	0.2199	0.0350	0.0269	2.0	1	1	0.12
DVR*	0.0111	0.7399	0.1290	0.4431	0.2902	0.4821	1.2	9.2042E−52	8.42E−09	0.25
PRR†	1.0000	1.0000	0.7373	0.5935	0.2395	0.0358	0.0	1	1.11E−09	0.01
LEW†	0.2312	0.0016	0.4557	0.1761	0.5580	0.2537	0.7	0.00356977	3.09314E−07	0.04
GGP†	0.3177	0.0474	0.2028	0.0675	0.7259	0.9003	1.1	1	3.66E−07	0.09
GVS†	0.3382	0.0112	0.0789	0.0086	0.2585	0.0889	1.8	1	6.52E−16	0.18
Skin										
GFS*	0.0389	0.0122	0.1908	0.4650	0.3245	0.8452	0.9	1.00E+00	0.003	0.01
WAT										
RTS*	3.81E−05	0.0140	1.78E−01	0.2543	7.44E−01	0.9329	3.7	1.37E−126	8.06E−144	0.44
GLT*	0.0030	0.0076	0.2748	0.3793	0.7942	0.9728	2.8	1.52E−103	4.15E−220	0.38
GSR*	0.0152	0.0117	0.4977	0.5711	0.4917	0.6185	4.0	9.82E−61	6.17E−184	0.60
SRT*	0.0345	0.0085	0.6589	0.0627	0.9935	0.9447	2.9	1.83E−10	4.98E−42	0.15
RLR*	0.0274	0.4889	0.2442	0.1496	0.8907	0.9639	1.5	1.64E−47	1.05E−35	0.32
GQS†	0.8348	0.8136	0.1286	0.0036	0.5974	0.7653	0.2	1.00E+00	1	0.00
GIL†	0.0736	0.5641	0.0147	0.6470	0.2998	0.5388	0.7	1.34E−107	0.018270	0.30
ILT†	0.3522	0.0771	0.2823	0.0164	1.0000	1.0000	0.2	9.78E−05	2.88E−18	0.03
MLS†	0.4198	0.0040	0.9952	0.9078	0.9564	0.2916	1.2	2.81E−132	9.73E−286	0.32
IRS†	0.5790	0.0098	1.0000	1.0000	0.9881	0.8501	0.8	2.28E−15	3.76E−103	0.16
PIR†	0.2232	0.0169	1.0000	1.0000	0.8907	0.3777	0.8	6.21E−49	2.96E−111	0.16
EGR†	0.0736	0.5641	0.0063	0.2776	0.0180	0.2702	0.7	4.35E−06	0.88	0.10
EAV†	1.0000	1.0000	0.7266	0.5724	0.1994	0.0240	0.0	1.00E+00	1	0.00
EGV†	0.9329	0.8717	0.4424	0.5746	0.3837	0.0491	0.2	1.00E+00	1	0.01
EGG†	0.2232	0.2114	0.4401	0.9739	0.0400	0.1030	0.7	8.52E−05	1.04E−12	0.09
VLV†	1.0000	1.0000	0.2823	0.2759	0.0898	0.0251	0.0	1.00E+00	1.05E−05	0.02
GHL†	0.5309	0.0190	0.7743	0.6751	0.8913	0.6569	0.6	0.85832081	0.054	0.03
LAL†	0.8119	0.0172	0.9860	0.7694	0.9026	0.5388	0.5	0.00113755	1.91E−38	0.08
GVL†	0.1568	0.3696	0.0497	0.6795	0.1089	0.8459	1.2	4.38E−08	3.17E−30	0.24
LVS†	1.0000	1.0000	0.0325	0.0830	0.1071	0.8163	0.0	0.49475029	1.98E−10	0.16
LKR†	0.8133	0.2031	0.7743	0.0164	1.0000	1.0000	0.3	0.7684612	7.56E−44	0.03
LLV†	0.5935	0.6737	0.1215	0.1153	0.0269	0.0631	0.2	1	1	0.06
QTR†	0.5935	0.7753	0.1852	0.0488	0.4480	0.4537	0.2	1	1	0.00
Muscle										
ELL*	0.0084	0.0317	0.2700	0.6445	2.83E−01	0.4954	1.3	2.7719E−52	3.16E−08	0.20
GVL*	0.0304	0.0080	0.0055	0.0846	2.12E−01	0.9599	1.8	0.50035796	4.03E−11	0.172966
DLL*	0.0421	0.0418	0.8750	0.9641	8.82E−01	0.9132	1.3	5.2143E−51	1.30527E−06	0.20
ASV*	0.0421	0.0033	0.0278	0.0639	1.79E−01	0.3887	1.3	0.30650945	1	0.15

Tripeptide sequences enriched in synchronous combinatorial selection in patients. For each tripeptide, *P*-values were calculated by Fisher's Exact test (one-sided) by comparison of its frequency in a target tissue with those in the unselected library or in the other tissues (combined) for the same round.
*tripeptides enriched in round 3 (*P*-value <0.05).
†tripeptides enriched in at least one round of selection (*P*-value <0.05).

Table S2. Candidate ligand-receptors identified through direct combinatorial selection in patients

Candidate ligand				Candidate receptor				
Target organ/ 7-mer peptide	Discovery approach	Protein ID	NCBI accession #	Discovery approach	Protein ID	NCBI accession #	Gene expression in target organ (EST / SAGE)	Ligand-receptor functional validation
Bone marrow								
CWNEWGQLC	protein array	protein phosphatase 1 regulatory subunit	NP_055145.3	affinity chromatography	Mannosyl-oligosaccharideglucosidase	NP_006293.2	yes / yes	n.d.
					CD98	NP_001012679.1	yes / yes	n.d.
CAHPSGEMC	similarity search	Chordin	NP_003732	affinity chromatography	complement C3	NP_000055.2	no / yes	n.d.
CRAHWATGC	protein array	Keratin-7	NP_005547.3	affinity chromatography	Radixin	NP_002897.1	yes / yes	n.d.
CGFQGSADC	protein array	plasticity-related gene 1 protein	NP_055654.2	affinity	TGF-beta-1	NP_000651.3	yes / yes	n.d.
		tripartite motif-containing protein 37	NP_001005207.1	chromatography				
		upstream stimulatory factor 2	NP_003358.1					
CSGEQLWKC	protein array	60S ribosomal protein L8	NP_000964.1	affinity	Cadherin-13	NP_001248.1	no / yes	n.d.
		histone deacetylase 2	NP_001518.2	chromatography	Cadherin-5	NP_001786.2	no / yes	
					Angiotensinogen	NP_000020.1	no / no	
CLAMPGGSC	protein array	BMP-binding endothelial regulator	NP_597725	affinity chromatography	Ezrin	NP_001104547.1	yes / yes	n.d.
CWKLGGGPC*	similarity search	advanced glycosylation end product-specific receptor	NP_001127.1	affinity chromatography	Leukocyte proteinase 3	NP_002768.3	yes / yes	yes
Skin								
CNSFGSGDC	protein array	p53 and DNA damage-regulated protein1 thyroid receptor-interacting protein 3	NP_110442.1 NP_004764.1	affinity chromatography	Integrin alpha-1	NP_852478.1	yes / yes	n.d.
WAT								
CSTRSGLTC	protein array	neurogenic differentiation factor 2 Coronin-1A	NP_006151.3 NP_009005.1	affinity chromatography	Nucleobindin-2	NP_005004.1	N.A. / N.A.	n.d.
CKGGRAKDC*†	similarity search	Annexin A2	NP_004030.1	similarity search	prohibitin	NP_002625.1	N.A. / N.A.	yes
Muscle								
CSTELVGEC	similarity search	Leptin	AAH69323	affinity chromatography	Aminopeptidase N	NP_001141.2	–	n.d.
CCTLLDGSSC	protein array	thyroid receptor-interacting protein 7	NP_004233.1	affinity chromatography	Integrin alpha-IIb	NP_000410.2	no / no	n.d.
		SEL1-like repeat-containing protein KIAA0746	NP_056002.2					
		round about -like protein 3	NP_071765.2					
CSAASVRRC	protein array	60S ribosomal protein L26	NP_000978.1	affinity chromatography	Aminopeptidase N	NP_001141.2	yes / no	n.d.
		60S ribosomal protein L11	NP_000966.2					
		60S ribosomal protein L26-like 1	NP_057177.1					
		phosphomevalonate kinase	NP_006547.1					
Tissue Shared								
CMGGHGWGC*	similarity search	integrin alpha-4	NP_000876.3	affinity chromatography	Annexin A4	NP_001144.1	–	yes
CMGGHGWGC*	similarity search	Cathepsin B	NP_001899.1	affinity chromatography	Apolipoprotein E3	NP_000032.1	–	yes

Putative ligand-receptors identified by direct combinatorial selection in patients. Whenever possible, the expression of the receptor candidate genes in the target organs was evaluated in silico by using Serial Analysis of Gene. Expression (SAGE) and Expressed Sequence Tags (ESTs) available in public databases (http://cgap.nci.nih.gov/SAGE). The dataset used contained bone marrow ($n = 44,841$ ESTs and 10,025,474 SAGE tags), skin ($n = 103,522$ ESTs and 169,106 SAGE tags) and muscle ($n = 201,788$ ESTs and 61,428,160 SAGE tags).

*peptides selected for validation. N.A.: not available in the database (SAGE/EST). N.D.: not determined.

Table S3. Vascular expression in a human TMA

	Expression in the vasculature	
Tissue ($n = 38$)	ANXA4	ApoE3
Hypothalamus / thalamus	yes	yes
Mammary gland	yes	yes
Placenta	yes	yes
Salivary gland	yes	yes
Skeletal muscle	yes	yes
Striatum	yes	yes
Substantia nigra	yes	yes
Umbilical cord	yes	yes
Bone marrow	yes	no
Choroid plexus	yes	no
Colon	yes	no
Dorsal root ganglia	yes	no
Heart	yes	no
Lymph node	yes	no
Prostate	yes	no
Skin	yes	no
Spleen	yes	no
Stomach/esophagus	yes	no
Thymus	yes	no
Cerebellum	no	yes
Liver	no	yes
Medulla	no	yes
Mesencephalon	no	yes
Sensory cortex	no	yes
Spinal cord	no	yes
Pituitary gland	no	yes
Adrenal gland	no	no
Brain stem	no	no
Kidney	no	no
Lung	no	no
Motor cortex	no	no
Pancreas	no	no
Small intestine	no	no
Temporal lobe	no	no
Thyroid	no	no
Appendix	no	N/D
Gall bladder	no	N/D
Pineal gland	no	N/D
Total (%)	19 out of 38 (50%) yes 19 out of 38 (50%) no	15 out of 38 (39%) yes 20 out of 38 (53%) no

N/D: not determined